Experimental investigations on heat transfer in transient boiling

Roberta Visentini, Catherine Colin, Pierre Ruyer

Proceedings of ASME 2012 Summer Heat Transfer Conference
July 8-July 12, 2012, Puerto Rico, USA

EXPERIMENTAL INVESTIGATIONS ON HEAT TRANSFER IN TRANSIENT BOILING

Roberta Visentini
IMFT, Toulouse University, France
IRSN, Cadarache, France
rvisenti@imft.fr

Catherine Colin
IMFT, Toulouse University, France
colin@imft.fr
Pierre Ruyer
IRSN, Cadarache, France
pierre.ruyer@irsn.fr

ABSTRACT

During reactivity initiated accidents in a core of a nuclear reactor, a power excursion occurs on some fuel rods. The consequent rapid boiling is a matter of study for the nuclear power plants safety evaluation, because of the risk for rod-clad failure. In order to better understand the influence of power excursions and to characterise the phases of the rapid boiling phenomenon, an experimental set-up has been built at the Institut de Mécanique des Fluides de Toulouse (IMFT). The test section is a semi annulus. The inner half cylinder is made of a stainless steel foil, heated by Joule effect. Its temperature is measured by an infrared camera filming the backside of the foil, coupled with a high speed camera for the visualization of the phenomena. Measurements were made when a square current signal is applied to the foil. They showed the influence of the supplied power and of the wall temperature increase rate during boiling.

NOMENCLATURE

dT/dt Temperature rate over time $[K/s]$.
T_L Liquid temperature $[°C]$.
T_{ONB} Temperature at the onset of nucleate boiling $[°C]$.
T_{NB} Nucleate boiling temperature $[°C]$.
T_{sat} Saturation temperature $[°C]$.
T_w Wall temperature $[°C]$.
I Current [A].
w Wall.

INTRODUCTION

In the core of a nuclear reactor, some control rods are located between the rods containing the nuclear fuel, see figure 1. These rods contain a neutron absorbing material which provides the control over the chain reaction. The design basis reactivity accident in pressurised water reactors is the rod ejection accident. This hypothetical accident consists of the failure of the control rod mechanisms housing. The consequences are a local fast rise in generated power and temperature of the nuclear fuel rods. It is called "Reactivity Initiated Accident" (RIA). The resulting power peak duration is only some milliseconds but it can lead to failure of the clad containing the nuclear fuel and release of radioactive material into the primary loop coolant. As a result the French "Institut de Radioprotection et de Sûreté Nucléaire" (IRSN), has been studying Reactivity Initiated Accidents (RIAs) for several years.

Clad to coolant heat transfer is a key phenomenon during RIA as it influences the clad temperature and, therefore, its mechanical resistance. Past research programs [1–3] have shown that the transient clad to coolant heat transfer in these accidental conditions highly differs from classical steady-state heat transfer correlations. Auracher and Marquardt [4] found that the critical heat flux becomes four-time higher than in the stationary case when the heating rate attains $50K/s$. In fast power transients, before the onset of boiling, the main mechanism appears to be conduction [5, 6], as this phase is too short to allow convective heat transfer. As the wall temperature increase is steep, boiling starts on a lot of nucleation sites at the same time which may explains the high value of critical heat fluxes. It has also been

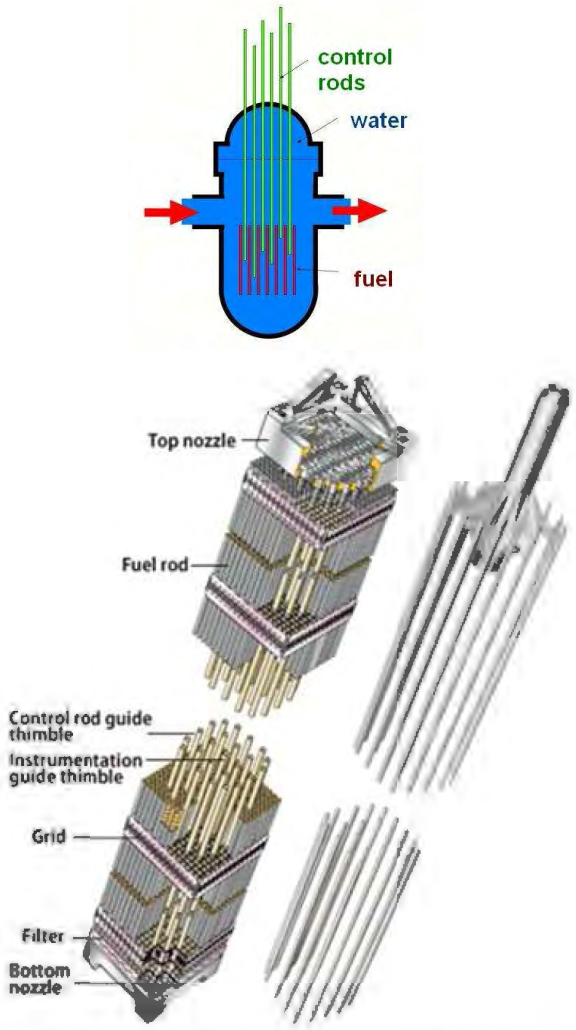

FIGURE 1. SCHEME OF THE CONTROL ROD SYSTEM.

shown that oxidation of the fuel rods can contribute to an enhancement of the critical heat flux [2].

It is possible to classify [7,8] the boiling transients based on the time spent in the nucleate boiling regime. While steady state boiling occurs for a nucleate boiling period of at least $500ms$, rapid transient boiling has a nucleate phase that lasts less than $100ms$. Once the boiling onset is reached, in rapid transient boiling, a vapor film covers the wall instantly. The nucleate boiling regime does not have time to be established. The boiling phenomenon becomes explosive when the nucleate boiling phase duration is around a hundred micro-seconds. Between the boiling onset and the film boiling onset in RIA conditions, only 20 to $50ms$ go by. The time needed for boiling bubbles to leave the wall is $4-20ms$ and some tens of bubbles are necessary to talk about fully developed nucleate boiling [9]. Thus, in the RIA boiling case, the nucleate boiling phase does not have enough time to be established. The film boiling phase is reached in a very short time. Currently there is no knowledge on the film development during rapid transient boiling. Some studies have shown that the wall surface conditions influences the re-wetting regime, and that they have more influence in this phase than in the boiling onset. Hysteresis appears and the critical heat flux is much lower in re-wetting than in heating. The re-wetting can be considered stationary, as the fuel rods have a considerable inertia and they do not cool quickly.

Sharp temperature increase is challenging experimentally. We could not find in literature analytical studies done at faster heating rates, except those on Joule heating, but they are affected by very high experimental uncertainties, and some experiences directly based on the RIA case [1], for the rod geometry. Hence, there is a great interest of building a rapid-heating experience that keeps the rod geometry and that gives more accurate results than previous tests.

In view of the absence of analytical experiments that investigate high heating rates, with a representative geometry and accurate measurement devices, and of the lack of knowledge on rapid transient boiling, an experimental set-up has been built at the "Institut de Mecanique des Fluides de Toulouse". In this article, the experimental apparatus and the measurement techniques are first described. Then, the evolution of the wall temperature is plotted, for the tests where the nucleate regime was established and for those where the film boiling was reached. The tendency of the boiling onset temperature, TONB, the mean nucleate boiling-regime temperature TNB and the film boiling thermal evolution are shown.

EXPERIMENTAL SET-UP AND MEASURMENT TECHNIQUES

The experimental set-up consists of a metal half-cylinder heated by Joule effect, placed in a half-annulus section. The inner half cylinder is made of a 50 microns thick stainless steel foil. Its diameter is $8.4mm$, and its length $200mm$. The outer part consists of a $34mm$ internal diameter glass half cylinder (fig. 2). The semi-annular section is filled with a coolant, named HFE7000. HFE7000 has been chosen because of its low saturation temperature ($34°C$ at atmospheric pressure), its latent heat of vaporisation (ten times smaller than the water one), and the reduction in the critical heat flux that it induces (for atmospheric pressure, the critical heat flux given by Zuber's correlation is $1.11MW/m^2$ for water and $0.17MW/m^2$ for HFE7000). It allows to reduce the required power to reach the transient boiling conditions.

The stainless steel has been chosen for its high resistivity ($72\mu\Omega m$). The resistivity and the reduced foil thickness allow to have a high electrical resistance and thus an elevated Joule power. The thickness homogeneity was verified by checking the homogeneity of the heated foil temperature by means of an

infra-red camera. The small thickness permits to consider that there is no temperature gradient across the foil (its Biot number is 0.018). The foil-thickness diffusion time, $0.6ms$, is actually small enough to assume that there is no time lag between the thermal evolution of the outer and inner wall. Thus, it is possible to measure the temperature of the wall that is in contact with the air, in order to know the temperature of the wall that is wetted. The metal half-cylinder is glued to two lateral quartz glass plates ($3mm$ thickness, $42mm$ width, $200mm$ length). The plates, together with the foil, are placed in an aluminum cell. In this cell, a visualization box is created in order to reduce optical distortions. There are windows on the back of the aluminum cell; they allow the electrical connections and the visual access to the metal foil. A special attention is paid to the electrical connections, as the contact resistance must be reduced. The electrical power that is dissipated in the foil is in average 85% of that of the whole system, including also electrical connections and connection cables. The electrical power is provided by a power supply *SORENSEN SGA*. It covers the $0-40V$ voltage range and the $0-250A$ current range. It can be used even at very low power, since it can supply even tension and current close to zero. The power supply is driven by an arbitrary generator where all kind of curves can be programmed. Thus, power peaks or gradual power ramps can be realised. The power supply can provide a current increase up to $45A/s$. Moreover, the thermal inertia of a fuel rod can be simulated by a smooth descent in the supplied power .

The metal foil is painted in black in order to increase its emissivity (the paint emissivity is 0.94). The thermal measurements are realized by means of an infra-red camera that looks at the foil from backward (see figure 2). It is a *CEDIP JADE III* camera and its sensitivity range is $3.5-5.1\mu m$. It has a focal plane array type and it has a Stirling-cooled MCT detector of $240\times 320 pixels^2$. An acquisition frequency of $1000im/s$ can be reached on small window of $64\times 120 pixels^2$ while, without windowing, its highest frequency is $350im/s$. The $1000im/s$ acquisition guarantees that the thermal dynamic is correctly followed, as the fastest heating tests have a $0.1s$ power rising time, and the diffusion time in the foil thickness is only $0.6ms$. The infrared camera is calibrated thanks to a *DCN 1000 N4* black body. It is possible to regulate a temperature level on this body and to film it by the camera. The uniformity of the black body surface with respect to the required temperature is guaranteed to be $0.3°C$ by the constructor, at $50°C$. Moreover, the declared temperature measurement accuracy is $\pm 0.01°C$ and the display resolution is $0.001°C$.

In the experiment that will be presented, a $50im/s$ frequency was chosen, with a $240\times 320 pixels^2$ window size. The metal foil area that was investigated was a $5\times 25mm^2$ rectangle.

The thermal measurements are coupled with high speed camera visualizations. The high speed camera, a *PHOTRON RS 3000*, is directed toward one side of the half cylinder. The used acquisition rate of the experiments was $500im/s$, with an image

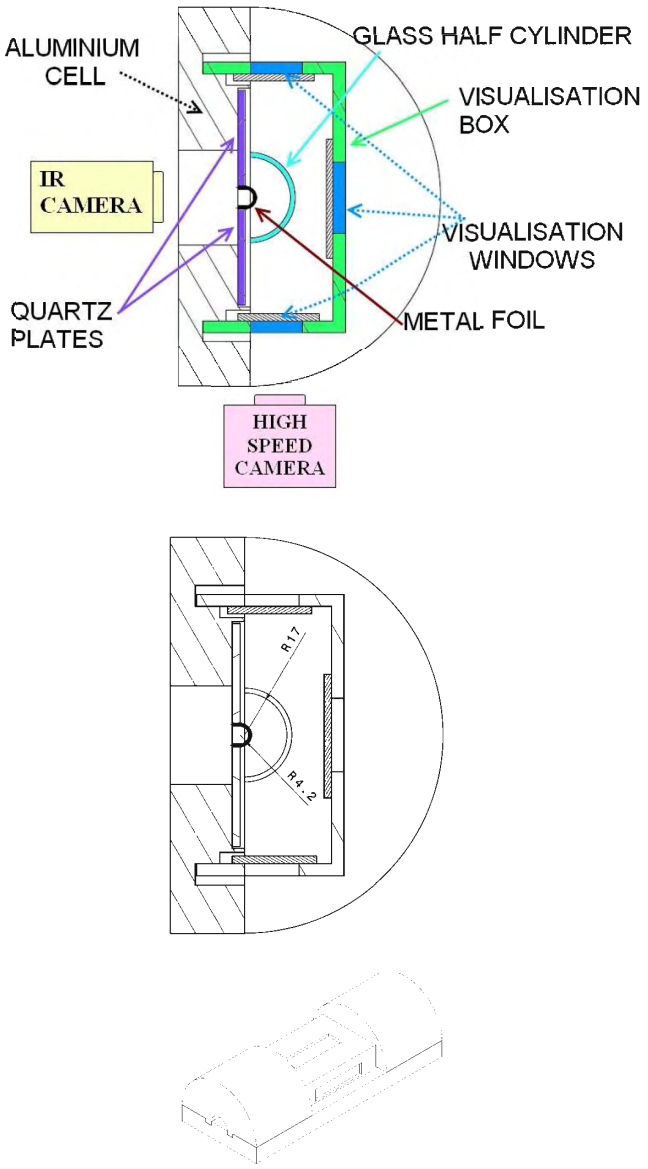

FIGURE 2. EXPERIMENTAL SET-UP.

size of $1024\times 1024 pixels^2$. Before the experimental tests, it is checked that the high speed camera visualization area is at the same height on the half cylinder that the infrared camera visualization zone (25mm). The output signal of the high speed camera is recorded by means of a *National Instruments* box. By the same box, the tension and current signals are picked up and this permits to synchronize the camera images to the recording of the other measurement signals.

The current signal is acquired by a *ITB 300-S LEM* sensor. It can measure up to $300A$ with a $\pm 0.05\%$ accuracy. It

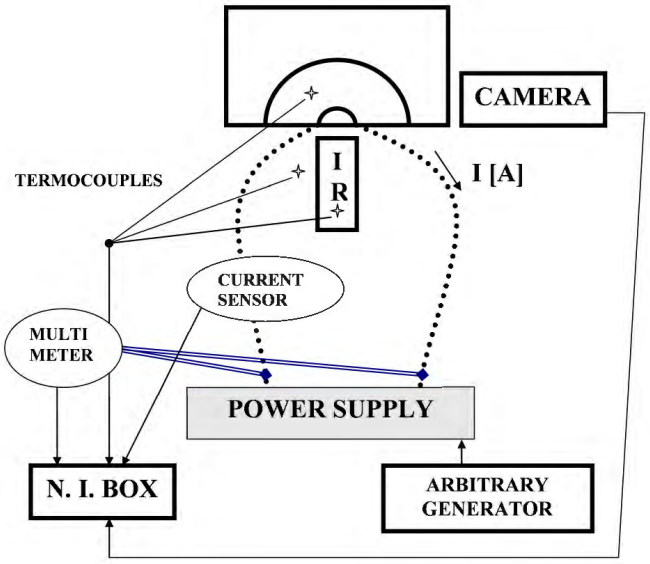

FIGURE 3. SCHEME OF THE MEASUREMENTS.

can follow current variations up to $100A/\mu s$ and its response time is lower than $1\mu s$ at $300A$. The sensor was calibrated by means of a 0.02% accuracy calibration instrument. The tension is measured by means of a *MY-64 multimeter* whose accuracy is $0.5\% + 1digit$ of the read value. Its calibration was done by means of a 0.02% precision sensor. The multimeter flexible cables allow a local voltage measurement, and thus the knowledge of the local electrical resistance of the metal foil. This measurement is done before the experiments. During the tests, the whole system tension is recorded, but it is possible to know the power that really passes through the foil by comparing the foil and the system resistances. The error on the power value is only 0.07%.

The *National Instruments* box is also used to acquire the thermocouples signals. There are three K-type thermocouples and they measure the HFE7000 temperature, the air temperature and the infrared camera temperature as well. The K-type thermocouples have a standard error between 2.2% and 0.75% and a $1.5°C$ tolerance in the investigated temperature range. Quantitative infrared measurements are possible only if the surroundings and the camera keep a constant temperature during the tests. The calibration of the infrared camera was made every time the surrounding temperature changed. This ensured to reduce the error on the thermal measurements. Figure 3 presents a scheme of the experimental set-up and measurement techniques.

RESULTS

In the experiments that will be presented in this article, a current square signal is employed. By means of the arbitrary generator, a current value is chosen and applied. The current signal

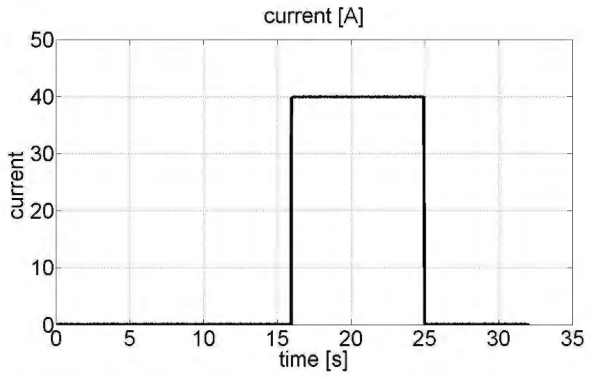

FIGURE 4. PROVIDED CURRENT SQUARE SIGNAL.

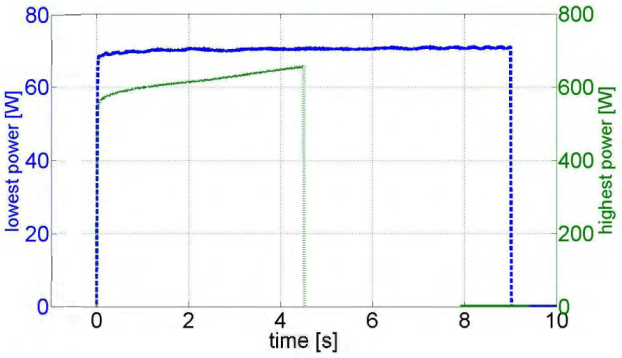

FIGURE 5. HIGHEST (GREEN, TEST 5) AND LOWEST (BLUE, TEST 1) POWER COMPARISON.

is shown in figure 4. It is possible to see that the current value is reached very rapidly and does not change in time. It is worth noting that it is not the power that is directly controlled. When the current is high and the experiment duration is short, the voltage value cannot stabilize. Moreover, as the applied voltage depends on the foil resistance, the foil temperature changes affect the provided power. This means that squared power signals are obtained only for low currents. This is the case of the blue curve in figure 5. Otherwise, the power curve tends to increase during the test. This can be seen in figure 5, green curve.

The lowest applied current value is $25A$. Under this minimum threshold nucleate boiling does not develop. This corresponds to a power of $70W$, measured at the exit of the power supply. By means of resistance measurements, it is possible to verify that 85% of the Joule power passes into the metal foils. The rest is lost into the electrical connections. This means that the power density is $2.25W/cm^2$ if the lateral heat losses are not taken into account. The highest imposed current value is $75A$, which corresponds to a mean power of $613W$ (that is $20W/cm^2$ on the foil surface without considering the lateral losses).

It is possible to identify two groups of experiments, that is,

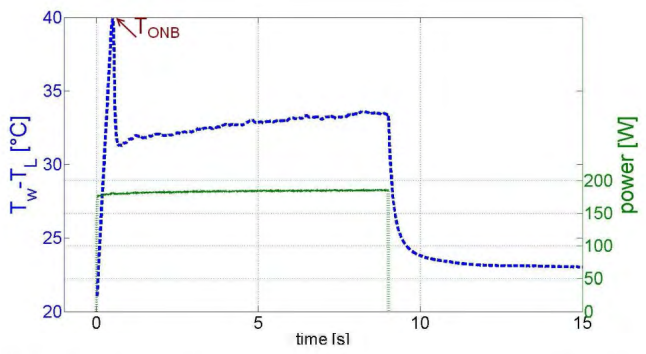

FIGURE 6. POWER AND TEMPERATURE TIME EVOLUTION; TEST 1, FIRST GROUP.

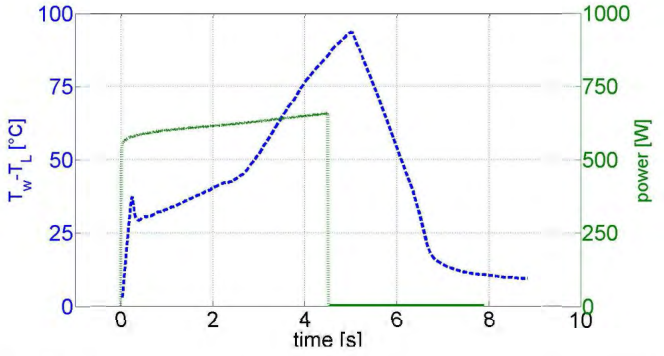

FIGURE 7. POWER AND TEMPERATURE TIME EVOLUTION; TEST 5, SECOND GROUP.

experiments whose power is lower than $300W$ and whose current is below $50A$, and experiments whose power and current values are higher than these two thresholds. For the first group, the output power signal can be considered squared, as the blue curve in figure 5. For the second one, the power cannot stabilize; this is the green curve case in the same figure. Considering the experiment duration, the first group experiments last $9s$, while the second group one are 4 or $5s$ long.

Three tests belong to the first group, and two to the second one. This division is due to the fact that each of these five tests was performed for a new IR camera calibration.

Considering the boiling phenomenon, in tests 1 to 3, that is the low power ones, a steady-state nucleate boiling is reached, with a constant or slightly increasing wall temperature. During the experiments that correspond to the tests 4 and 5, whose applied power is higher, a transition to film boiling occurs. Moreover, the nucleate boiling regime is transient. As the provided power is elevated, the boiling phenomenon evolves rapidly from nucleate boiling into film boiling. A transition to the film boiling condition is clearly observed in test five.

The difference between the two groups of experiments is clearly visible in figure 6 and figure 7. There, the power curve is plotted together with the resulting foil wall temperature. The temperature information comes from the infrared measurements. In fact, it is possible to plot the temperature time evolution by means of the infrared measurements.

On the infrared pictures, a homogeneous area which covers the metal foil surface is considered. It is important not to take into account the borders of the metal foil and to focalise on the central part. Border temperatures are very high, while the curvature effect may alter the measurements far from the center of the half cylinder. The considered window is $3mm$ large and $10mm$ long (vertical direction). Its size is big enough to allow a mean spatial temperature evaluation. When the fluid is boiling, the average temperature gradient in the considered area is less than $4°C$. This is due to the fact that the nucleation sites have a

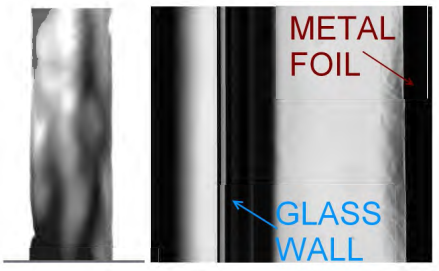

(a) *IR CAMERA IMAGE* (b) *HIGH SPEED CAMERA IMAGE.*

FIGURE 8. THERMAL PLUMES ON THE METAL FOIL.

lower temperature than the surrounding points. The temperature inhomogeneity in the considered area of the infrared images is $1°C$ during the first liquid phase.

Actually, these figures 6 and 7 present the wall-liquid temperature difference $T_w - T_L$. The mean fluid sub cooling during these experiments, $T_{sat} - T_L$, is $7°C$ for the low power case (fig. 6) and $6-7°C$ for the high power one (fig. 7).

Figure 6 presents the low power case. It is possible to see that there is a high increase in the temperature value during the first $0.5s$. The power passes from zero to the peak value in $30ms$. The metal foil follows this rapid increase and gets $20K$ in less than a second. This corresponds to the single-phase heat transfer regime, before the boiling onset. Infrared measurements and high speed camera images confirm that there are thermal plumes into the fluid. The infrared camera frequency, that is $50Hz$, allows to follow the temperature increase. Figure 8 shows a high speed camera image and an infrared image where thermal spirals clearly appear. The highest temperature of the wall temperature plot (fig. fig.PTLOW), corresponds to the boiling onset (T_{ONB}). As boiling begins, the heat transfer is enhanced, so the wall temperature decreases considerably. The following part of the boiling temperature evolution in time curve corresponds to an almost constant temperature. It is the nucleate boiling heat trans-

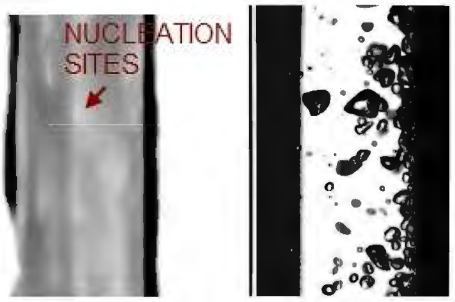

(a) *IR CAMERA IMAGE* (b) *HIGH SPEED CAMERA IMAGE.*

FIGURE 9. NUCLEATE BOILING ON THE METAL FOIL.

FIGURE 10. FILM BOILING ON THE METAL FOIL, IR CAMERA IMAGE. THE VAPOUR FILM APPEARS FROM THE RIGHT CORNER.

fer that avoids the increase of the wall temperature. Figure 9 shows an infrared image where nucleation sites appear. The second image of the same figure presents nucleate boiling as seen by the high speed camera. The small augmentation that can be seen in the temperature evolution corresponds to the power small increase. Finally, as the power is switched off, the temperature decreases rapidly. Once again, the small inertia of the metal foil makes it respond instantaneously to the power signal.

Figure 7 shows the case of a higher power that leads to film boiling. The single-phase heat transfer, that is, before the boiling onset, and the nucleate boiling regime last less than in the previous tests. The nucleate boiling regime is not established. Temperature grows all the test long, even during nucleate boiling. The film boiling set-up corresponds to a change in the slope. The point of slope change should correspond to the onset of a film boiling regime.

Infrared camera images show that the film begins to develop from the top of the metal foil. This is what can be seen in figure 10.

The experiments are interrupted before that the high temperature damages the metal foil. It is possible to see that there is a delay in the cooling process. This is due to the high temperature reached and probably to the fact that the quartz plates are heated as well. They have a higher inertia than the metal foil, and they

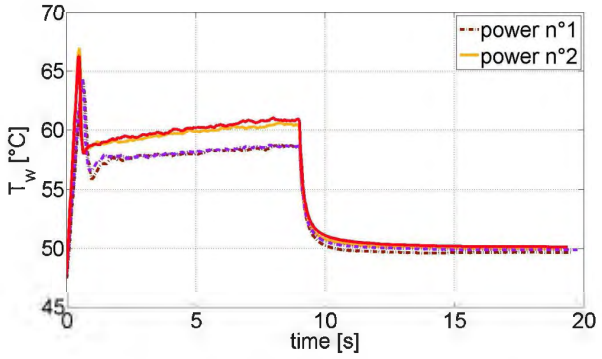

FIGURE 11. MEASUREMENTS REPEATABILITY, TEST 1 AND 2.

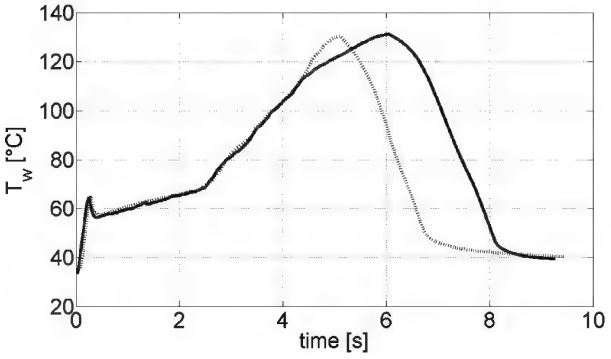

FIGURE 12. MEASUREMENTS REPEATABILITY, TEST 5. THE EXPERIMENT DURATIONS ARE 5*s* AND 5.5*s* AND THE SAME POWER IS APPLIED.

need more time to cool down. The temperature enhancement is still partly caused by the power increment, but it is mainly due to the heat transfer worsening. The vapor film deteriorates the heat transfer between the wall and the fluid.

Repeatability of the tests is shown in figure 11. Two sets of curves are presented: they belong to tests one and two. Figure 12 presents two experiments, having the same power, and belonging to the fifth series. The repeatability of the experiments guarantees that data are consistent.

It is worth noting that a numerical simulation model has been developed in order to evaluate the amount of the heat losses and to know the heat flux transmitted to the fluid. The Fourier equation is solved for the metal foil and quartz plates, using the *Comsol Multiphysics* software. This allows a more quantitative data treatment. The numerical simulations are under development.

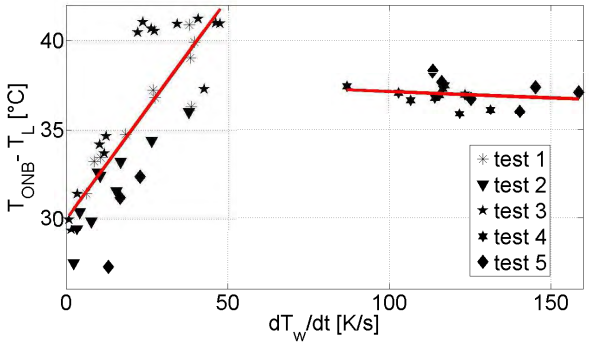

FIGURE 13. $T_{ONB} - T_L$ VERSUS TEMPERATURE INCREASE RATE.

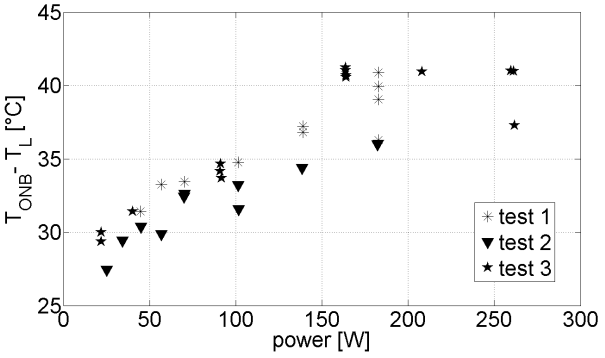

FIGURE 14. $T_{ONB} - T_L$ VERSUS SUPPLIED POWER, ZOOM ON TESTS 1 TO 3.

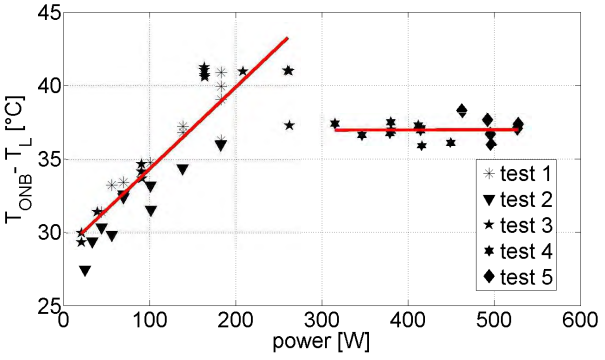

FIGURE 15. $T_{ONB} - T_L$ VERSUS SUPPLIED POWER.

Result Analysis

In the following part, tests are compared in order to highlight the most significant tendencies. When one of the plotted parameter is the power, it means the power that is produced by the electrical supply. The current and voltage output measurements allow the supplied power evaluation. In order to know the real heat flux that is passed from the metal foil to the fluid, it is necessary to take into account the thermal losses. The metal foil support is also heated by the Joule power, so this amount of energy that does not go to the fluid, has to be subtracted from the whole power, in order to evaluate the heat flux. Simulations of the experimental set-up are thus needed and planned for the near future.

The first interesting point is the boiling onset. The boiling onset temperature, T_{ONB}, is the highest temperature that is reached before the nucleate boiling regime begins. This temperature is referred as T_{ONB} in figure 6. As nucleate boiling starts, bubbles appear and they allow a more efficient heat transfer mechanism, because of the phase change, so the wall is cooled down. The boiling onset temperature, T_{ONB}, is plotted in figure 13, figure 14 and figure 15. Since the liquid temperature varies during the tests, the difference $T_{ONB} - T_L$ is plotted.

Figure 13, shows how the onset boiling temperature, T_{ONB}, is influenced by the temperature increase slope, dT_w/dt. The dT_w/dt value is evaluated for the single-phase heat transfer regime, taking into account the beginning temperature and the T_{ONB} value. It is possible to see that the two main groups (that is, test 1, 2 and 3 against 4 and 5) behave differently. Tests 1 to 3 present a linear increase of the T_{ONB} as a function of the dT_w/dt. The single-phase heat transfer is enhanced when the temperature increase rate dT_w/dt grows. Thus, the beginning of boiling is delayed. The fourth and fifth tests do not follow the same tendency. It seems that $T_{ONB} - T_L$ reaches an asymptotic value, independent of the temperature increase rate. The fitting line is almost horizontal. The two groups division occurs at $60K/s$ heating rate. It is possible to estimate the nucleation site radius [10] for a $T_{ONB} - T_L$ value of $37K$, that is, the asymptotic value. This gives $2 \cdot 10^{-2} \mu m$. Probably all the nucleation sites, even the smaller ones, are activated, which explains the asymptotic behavior.

The same behavior can be seen on figure 15. There, the temperature is plotted versus the Joule power. The two groups are clearly divided. Figure 14 is a zoom on the first three tests. The asymptotic tendency is kept by tests 4 and 5. This is due to the proportionality between the Joule power and the temperature increase rate dT_w/dt. The curve that fits the data has the following form:

$$dT_w/dt[°C] = 0.3 \cdot power[W] - 13.79 \quad (1)$$

Let us consider the nucleate boiling part. The mean temperature of the nucleate boiling phenomenon is plotted versus the mean power on the same time lap, in figure 16. The two groups still have different behaviors. The tests belonging to the first category, that is, those where the nucleate boiling phase is well established, can be described by a tendency line which is

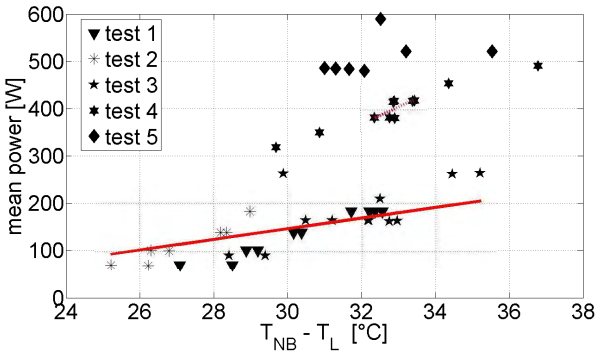

FIGURE 16. T_{NB} VERSUS SUPPLIED MEAN POWER.

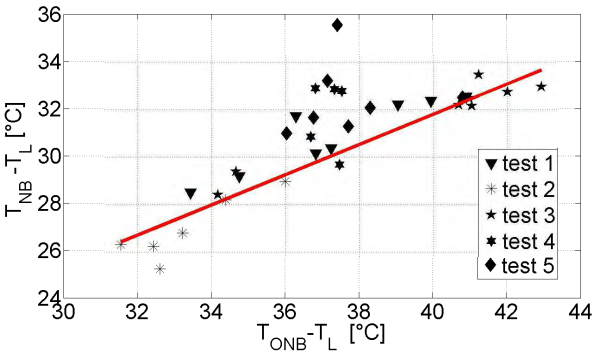

FIGURE 17. T_{NB} VERSUS T_{ONB}.

parallel to that of the second group. In fact the fitting line slope is $0.0152W/K$ for tests 1 to 3 and $0.0170W/K$ for tests 4 and 5. A deeper analysis is needed to make a qualitative comparison to the data of Auracher and Marquardt [4].

It is in fact necessary to calculate the slope of the nucleate boiling temperature. The first test group slope is between $5 \cdot 10^{-2} K/s$ and $0.5K/s$. Thus, the temperature can be considered constant. For the fourth test the slope passes from 1, for the lower power belonging to this test, to $4K/s$. The fifth test presents a slop from 4.7 to $9K/s$. Auracher and Marquardt plotted the heat flux density versus the wall superheat using the temperature increase rate as parameter. It means that the variation of the temperature increase rate leads to different boiling curves. According to this statement, the points belonging to tests 1 to 3 can be considered on the same boiling curve. This curve is not very steep as the temperature increase rate is almost zero. The boiling regime can thus be considered steady. This is consistent with what is found by Auracher and Marquardt [4]. Points belonging to tests 4 and 5 cannot be collected on the same curve, because of the variation of the temperature increase rate. It is possible to plot a curve for some experiments of the fourth test (fig. 16). The temperature increase rate being higher than for the first group tests, the slope is steeper. This is consistent with Auracher and Marquardt's results.

Auracher and Marquardt controlled the temperature increase and went up to $50K/s$, but the lowest curves correspond to the temperature rates that are present in tests 4 and 5. A quantitative comparison will be possible when the numerical heat transfer simulation will allow to know the heat flux density. In fact it is possible to know the Joule power by means of the tension and current measurements, but the flux that passes from the heated wall to the fluid is still unknown. The quartz plates do not have an elevated thermal conductivity but there is a part of the supplied power that is transmitted through them. In a first evaluation, it seems that around 30% of the total heat flux may be lost into the quartz plate, but it is necessary to throw light on these losses. However, if the lateral heat losses are considered as the 30% of the Joule power passing into the metal foil, it is possible to estimated the heat flux density of the tests. It is of the same order as the value of Auracher and Marquardt's lowest curves.

In figure 17 the mean boiling temperature is plotted versus the temperature of boiling onset. The two test groups are still separated. Tests 1 to 3 present a linear proportionality between the two temperature. That is, as the $T_{ONB} - T_L$ value grows, the T_{NB} value grows as well. Considering figure 14, it is possible to see that the same tendency that can be found plotting $T_{ONB} - T_L$ versus power, is present when T_{NB} is plotted versus $T_{ONB} - T_L$. This is consistent with the proportionality between power and mean nucleate boiling temperature.

Tests 4 and 5, on the contrary, show a vertical asymptote. That is, the boiling temperature T_{NB} keeps growing while the T_{ONB} does not. The asymptote is at $T_{ONB} - T_L \approx 37°C$. This behavior is understandable taking into account the fact that the boiling onset is not affected by a power increment, while the nucleate boiling temperature is. Once again, the effect of power on the nucleate boiling temperature is reproduced in this figure as well.

CONCLUSION

An experimental set-up has been built to investigate fast transient boiling regimes that can be encountered in the case of an hypothetical reactivity-initiated nuclear accidents. A semi annular metallic foil is heated by Joule effect. The foil temperature evolution is recorded with an infrared camera. Different power steps are applied to the foil. A rapid increase in the wall temperature is observed until the onset of nucleate boiling occurs. Then the wall temperature quickly decreases and stabilizes around a steady value in the nucleate boiling regime. At high power steady nucleate boiling is not observed, the wall temperature always increases and it is possible to see a transition to film

boiling. Since the metallic foil is glued to quartz plates, a part of the power could be lost by conduction toward the plates and the heat flux transmitted to the liquid cannot be directly evaluated. Thus the unsteady Fourier equation has to be solved numerically to quantify this heat flux.

The first results are presented in this paper versus the Joule power that is supplied by the electric supplier. The more the power increases, the more the wall temperature increase dT_w/dt augments. The temperature at the onset of nucleate boiling directly increases with dT_w/dt until it reaches a maximum value associated to the activation of the smallest nucleation sites on the foil. The evolution of the wall temperature during nucleate boiling is also plotted, versus the mean power for steady and transient nucleate boiling regimes. The heat transfer is much larger in transient regime as already observed by other authors.

In the near future, a numerical simulation of the heat transfer within the metal foil and toward the quartz plates, will be ran. Thus, a quantitative comparison with literature results will be possible. Moreover, different test cases, like linear power increase tests or tests where the film boiling is instantaneously reached will be performed. This last type of experiments will hopefully clarify the mechanism of boiling when rapid power increase is supplied to the wall.

ACKNOWLEDGMENT

The authors would like to acknowledge the technical staff of IMFT, especially Laurent Mouneix, for building the experimental set-up. Sebastien Cazin is also greatly thanked for his support in the infrared measurements and the flow visualizations.

REFERENCES

[1] Bessiron, V., Sugiyama, T., and Fuketa, T., 2007. "Clad to coolant heat transfer in NSRR experiments". *Journal of Nuclear Science and Technology,* ***44***(5), January, pp. 723–732.

[2] Sugiyama, T., and Fuketa, T., 2004. "Effect of cladding surface pre oxidation on rod coolability under reactivity initiated accident conditions". *Journal of Nuclear Science and Technology,* ***41***(11), November, pp. 1083–1090.

[3] Beloeil, L., 2000. "Etude d´ un accident de criticité mettant en présence des crayons combustibles et de l´ eau hors réacteur de puissance". Master's thesis, Universit d´ Aix-Marseille I - Institut Universitaire des Systèmes Thermiques Industriels.

[4] Auracher, H., and Marquardt, W., 2002. "Experimental studies of boiling mechanisms in all boiling regimes under steady state and transient conditions". *Int. J. Therm. Sci.,* ***41***(1), February, pp. 586–598.

[5] V. I. Deev, H. Lwin, V. S. K. K. V. K. A. A. L., 2007. "Critical heat flux modeling in water pool boiling during power transients". *International Journal of Heat and Mass Transfer,* ***50***(19), September, pp. 3780–3787.

[6] Wang, J., 2000. "Preliminary analysis of rapid boiling heat transfer". *International Communications in Heat and Mass Transfer,* ***27***(3), April, pp. 377–388.

[7] A. Sakurai, M. Shiotsu, K. H., 1987. "Transient boiling caused by vapor film collapse at minimum heat flux in film boiling". *Nuclear Engineering and Design,* ***99***(1), February, pp. 167–175.

[8] Derewnicki, K., 1985. "Experimental studies of heat transfer and vapour formation in fast transient boiling". *International Journal of Heat and Mass Transfer,* ***28***(11), November, pp. 2085–2092.

[9] Sakurai, A., Shiotsu, M., Hata, K., and Fukuda, K., 2000. "Photographic study on transitions from non boiling and nucleate boiling regime to film boiling due to increasing heat inputs in liquid nitrogen and water". *Nuclear Engineering and Design,* ***200***(1), September, pp. 39–54.

[10] Carey, V. P., 1992. *Liquid Vapor Phase Change Phenomena, An introduction to the thermophysics of Vaporization and Condensation Processes in heat Transfer Equipment.* Series in Chemical and Mechanical Enginnering, Taylor and Francis, Hebron, KY.